

Durability and Reliability Improvement Pathways for Thermosyphon Solar Collectors

**B.3. Report on durability and reliability
improving research and technical
results**

Durability and Reliability Improvement Pathways for Thermosyphon Solar Collectors

Deliverable

Subtask B. Thermosyphon Systems

Report B.3. Report on durability and reliability improving research and technical results

A SHC Task 69: Solar Hot Water for 2030 Report

Editors:

Li Bojia (CABR), Li Haimeng (CABR)

Contributing Authors (in alphabetical order):

Bian Mengmeng (CABR), Robert Stayton (Cabrillo College), Zhang Xinyu (CABR)

Date June 10, 2026

Report number: B.3 DOI: 10.18777/ieashc-task69-2026-0003

The contents of this report do not necessarily reflect the viewpoints or policies of the International Energy Agency (IEA) or its member countries, the IEA Solar Heating and Cooling Technology Collaboration Programme (SHC TCP) members or the participating researchers.

Contents

Contents	ii
1 Executive Summary	1
2 Introduction	3
3 Durability and Reliability Improving Research	5
3.1 Ageing Test under Exposure Conditions	5
3.1.1 Introduction.....	5
3.1.2 Ageing Process of Evacuated Tube Solar Collectors	5
3.1.3 Specification for Tested Solar Collector.....	5
3.1.4 Test Method.....	6
3.1.5 Test Conditions.....	6
3.1.6 Thermal Performance Test Result.....	7
3.1.7 Conclusion.....	8
3.2 Overheating Control	8
3.2.1 Introduction.....	8
3.2.2 Main Research.....	8
3.2.3 Development Direction	10
3.3 Mitigate Heat Loss.....	10
3.3.1 Introduction.....	10
3.3.2 Main Research.....	11
3.3.3 Development Direction	14
3.4 Freeze Protection.....	15
3.4.1 Introduction.....	15
3.4.2 Main Research: Applications of Supercritical CO ₂ Fluids.....	15
3.4.3 Main Research: Passive Freeze Protection.....	18
3.4.4 Development Direction	20
3.5 Loop Thermosyphon Technology	21
3.5.1 Introduction.....	21
3.5.2 Main Research.....	21
3.5.3 Development Direction	24
4 Technical Solutions	25
4.1 Technical Solutions for Component Installation and Fixation	25
4.1.1 Anti-Vibration Support System Design.....	25
4.1.2 Installation Solutions for Component and Safety Devices	25
4.2 Multi-layered Protection System.....	25
4.2.1 Overheating Protection	25
4.2.2 Frost Protection	26
4.2.3 Comprehensive Corrosion Protection Solutions	26
4.2.4 Intelligent Insulation System Design	26
4.3 Intelligent Monitoring and Predictive Maintenance Systems	27

4.3.1	Monitoring Platform Development.....	27
4.3.2	Implementation of Predictive Maintenance Strategies	27
5	Conclusion.....	27
6	Appendix.....	29
6.1	Abbreviations	29
6.2	List of Figures.....	29
6.3	List of Tables.....	31
6.4	References.....	31

1 Executive Summary

The core objective of this report is to conduct an in-depth investigation into the real-world durability and reliability challenges faced by users of *thermosyphon solar collectors* across different regions globally, particularly within the coverage areas of the Global Sustainable Energy Centers Network. By examining cutting-edge research and technological developments, it aims to provide practical solutions for addressing critical issues such as thermal shock, overheating, leakage, and freezing. This section summarizes the latest developments and cutting-edge technologies related to these issues.

Several reports have highlighted the key reliability and durability issues and pathways to overcome these.

Aging and Corrosion

Aging exposure tests indicate that the hardening of rubber sealing rings and the degradation of insulation materials are primary causes of increased heat loss over time. These findings underscore the importance of material selection and structural design in collectors, as well as the essential role of long-term durability testing in quality control. To combat corrosion, strategies such as continuous chloride ion monitoring, the use of corrosion-resistant materials (e.g., duplex stainless steel and titanium), and the maintenance of cathodic protection systems—combining sacrificial anodes with impressed current—have been proposed.

Overheating Protection and Heat Loss

Related scholars have proposed an innovative overheating restriction strategy based on precise adjustment of the working fluid inventory in heat pipes. By minimizing fluid filling and intentionally operating near the 'dry limit' to achieve self-limiting thermal protection. This passive form of regulation requires no external energy or control, effectively balancing efficiency with safety. It reduces thermal stress on the system, prolongs the lifespan of key components, and offers a cost-effective and reliable engineering solution to overheating. Regarding the issue of heat loss, phase change materials integrated into the tank or collector help minimize nighttime heat loss, acting as a "thermal battery" to improve energy efficiency and user experience.

Freeze Protection

To prevent freezing and corrosion in cold climates, loop thermosyphon technology has been introduced. It uses a freeze-resistant working fluid in the collector loop, achieving physical isolation from the water system and heating stored water indirectly via a heat exchanger. Another approach involves the use of supercritical carbon dioxide as a working fluid in thermosyphon vacuum tube collectors, which could enable operation in extremely cold regions. A dual-circuit passive antifreeze system offers another option, avoiding the complexities of antifreeze fluids and electrical controls.

Installation and Maintenance

System reliability and durability can also be enhanced through improved installation, protection, and operational practices. Anti-vibration support systems and thermal displacement compensation technology—through elastic damping design, precise bracket arrangement, and compensator selection—help mitigate mechanical vibrations and thermal stress. Intelligent insulation and corrosion prevention measures further contribute to system longevity. Moreover, intelligent monitoring platforms based on multi-sensor networks can employ machine learning models for condition assessment and fault prediction. This supports a predictive maintenance strategy based on equipment health indices, shifting the paradigm from scheduled to on-demand maintenance.

As shown in Figure 1, the failure rate of a solar water heating system typically evolves through three distinct phases. In initial failure period, failures during this stage are mainly caused by design flaws, manufacturing defects, improper installation, or operational errors. Strengthening quality control and implementing standardized installation procedures can effectively reduce the early failure rate and improve initial reliability. For example, adopting a thermosyphon loop design helps overcome freezing and corrosion issues common in traditional systems, thereby enhancing durability. During random failure period, the system operates stably with a low and steady failure rate, representing its useful life period. Failures in this phase are usually due to irregular maintenance or accidental operational mistakes. To extend the useful life, measures such as overheating protection and the use of phase-change materials to reduce nighttime heat loss can improve daily operational reliability. Additionally, in extremely cold climates, studies suggest using new types of heat-transfer fluids or dual-cycle passive freeze protection to ensure reliable operation under severe weather conditions. In the wear-out failure period, after prolonged operation, wear and corrosion of components gradually increase the failure rate. During this stage, regular inspections, continuous monitoring, and data analysis are essential to predict degradation trends and schedule proactive maintenance.

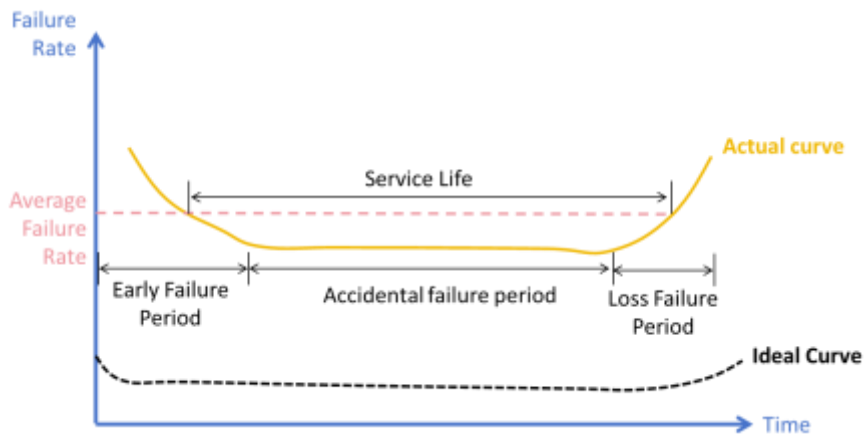


Figure 1: Typical product failure rate curve.

In summary, this report systematically integrates and applies relevant research findings to advance the overall performance, lifespan, and reliability of solar water heating systems. To achieve this, the study focuses on practical solutions for key challenges identified across different global regions.

2 Introduction

As an efficient and environmentally friendly solution for supplying hot water, thermosyphon solar water heaters have been installed around the world. As the largest solar thermal market, there were 477.8 million m² solar collectors installed in China in 2017. In addition, evacuated tube collectors account for about 90% of the market share.

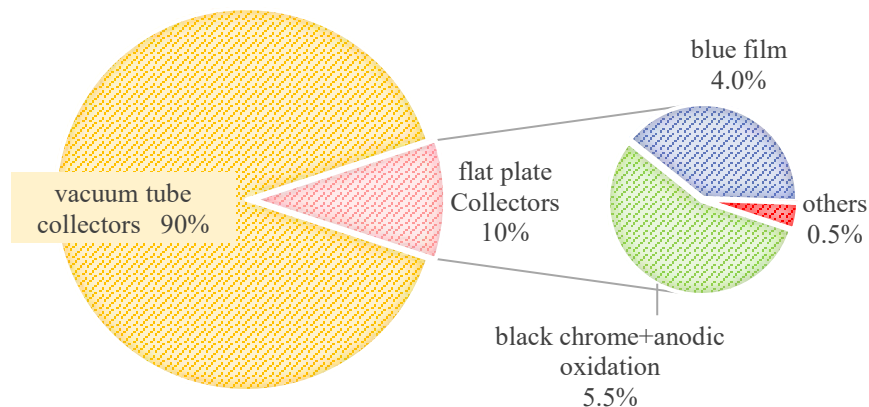


Figure 2: Market Share of ETC and FPC in China.

Reliable thermosyphon solar collectors can only be realized through a multidisciplinary technical approach which integrates advanced materials science, chemical engineering, structural mechanics, intelligent control, and manufacturing expertise. Current global R&D efforts have proposed many innovative solutions in research years to enhance their long-term performance under demanding operating conditions. At present, industry is shifting from conventional passive protection toward active prediction, intelligent regulation, and durability-oriented design to meet growing market expectations for energy efficiency, service life, and operational reliability. Significant progress has been made in addressing critical challenges such as aging, corrosion, overheating protection, heat loss and freeze protection, improving product adaptability and longevity in diverse environments.

Notable advancements have been achieved in corrosion and leakage prevention through a multi-tier protection strategy encompassing substrate, coating, and system-level defenses. The adoption of high-performance alloys—including ultra-low-carbon duplex stainless steels (SUS444, SUS3042B) and titanium—has improved resistance to chloride-induced pitting and stress corrosion cracking. Surface protection technologies have also advanced through innovations such as graphene coatings, nano-scale self-cleaning coatings (via sol-gel processes), and high-density enamel layers, all contributing to reduced corrosion rates and scale adhesion. A structural breakthrough is exemplified by Gemeiqi's "Jingmei Inner Tank," which utilizes a three-layer seamless construction: a food-grade polymer inner liner, a micron-level silicon-based reinforcement layer, and a resin-composite outer shell. This weld-free design eliminates traditional leakage risks associated with welded seams and has endured over 2 million pulse pressure cycles with a pressure rating exceeding 3 MPa. System-level protections—such as magnetic filtration and corrosion inhibitor injection—further enhance water quality management and corrosion resistance.

In overheating and thermal shock protection, integrated mechanical and electronic control strategies have set new benchmarks. Mechanical temperature and pressure relief valves (T&P Valves) remain critical fail-safes, while AI-driven algorithms using multi-sensor data (temperature, flow, pressure) enable predictive thermal management. LSTM neural networks learn usage patterns to preemptively adjust heating parameters, mitigating localized overheating, and enhancing component durability. Compliance with the updated safety standard GB 4706.23-2022 requires operational stability within $\pm 3^{\circ}\text{C}$ under $\pm 10\%$ voltage fluctuation. To counter thermal shock, bypass mixing valves regulate water temperature automatically, avoiding direct exposure of valves to high-temperature flows—thus reducing thermal stress. Solar thermal systems also incorporate enhanced overheat protection, with pressure relief devices activating within 120 seconds and steam discharge temperatures calibrated to $99 \pm 2^{\circ}\text{C}$ in simulated stagnation conditions.

Innovations in materials and freeze-protection technologies are reshaping system durability and low-temperature performance. Phase change materials (PCMs), particularly nano-encapsulated composites, are integrated into storage and heat exchange units to buffer thermal load variations, leverage off-peak electricity, and minimize cycling damage. In solar thermal applications, freeze resistance has been significantly improved. Tongling Hong'an Solar's anti-freeze vacuum tube design incorporates heating elements at the tube base to ensure uniform thermal distribution in cold conditions. Xingya New Energy's patented "Self-Actuated Phase-Change Vaporizing Flat-Plane

Solar Water Heater” employs a sealed copper tubing system with a phase-change medium, eliminating external contact, preventing scaling, and delivering reliable low-temperature operation. Beijing Solar Energy Research Institute’s “All-Vacuum-Tube Winter Water Heater” uses siphon-driven drainage to clear pipes of cold water, offering a robust solution for year-round operation in freezing climates.

System intelligence and control strategies continue to advance toward adaptive, high-efficiency operation with strengthened protection against thermal shock, overheating, and freezing. Optimization algorithms—including genetic algorithms (GA) and artificial neural networks (ANN)—enable dynamic modeling of thermosyphon flow to maximize the coefficient of performance (COP). Hardware enhancements such as sealed convective designs, turbulence-optimized flow paths, and low-resistance valves reduce hydraulic losses and improve thermal efficiency. Intelligent control systems adjust operational parameters in response to ambient and load changes, balancing energy efficiency with reliability. For freeze protection, distributed temperature sensors trigger anti-freeze circulation or heating modes when critical thresholds are breached. Gradient temperature control and flow modulation minimize thermal stress during transient operation, extending system service life.



3 Durability and Reliability Improving Research

3.1 Ageing Test under Exposure Conditions

3.1.1 Introduction

Thermosyphon solar collectors should be designed for long-term exposure to high levels of solar irradiation and high temperature. However, most collectors are only evaluated for their thermal performance before and after exposure. To address this, an ageing test was recently conducted by the China Academy of Building Research. In this test, four types of solar collectors were assessed, including: Flat-plate collector (FPC), Glass-metal sealed evacuated tube collector (GSETC), Heat pipe evacuated tube collector (HPETC), U-type evacuated tube collector (UETC) for the comparison of FPC and ETC.

3.1.2 Ageing Process of Evacuated Tube Solar Collectors

Under solar radiation and temperature change, the rubber ring would harden, which led to the joint gap between tubes and manifold becoming large, resulting in more heat loss. In addition, after exposure the insulation material's performance would weaken, which reduces the thermal performance.

To investigate performance changes under exposure conditions, several kinds of ETC were selected to conduct the aging test. FPC had also been tested for comparison. All the work had been carried out by the National Center for Quality Supervision and Testing of Solar Heating Systems (Beijing).



Figure 3: Images of Some ETCs after Exposure.

3.1.3 Specification for Tested Solar Collector

Selected solar collectors were used commonly in China. Four types of solar collectors were tested, including Flat-plate collector (FPC), Glass-metal sealed evacuated tube collector (GSETC), Heat pipe inside evacuated tube collector (HPETC), U type evacuated tube collector (UETC).

Detailed information of FPC in Table 1, others in Table 2.

Table 1: Specification of Tested Flat Plate Solar Collector.

Cover Material	4 mm glass
Layers of Cover	Single
Absorber Material	Black Chrome
Aperture Dimension	1950mm X 940mm
Aperture Area	1.83m ²
Gross Area	2.00m ²

Table 2: Specifications of The Tested Evacuated Tube Collectors.

Solar Collector	GSETC	HPETC	UETC
Array of Tubes	Vertical	Vertical	Vertical
Number of Tubes	8	16	16
External Diameter of Cover Tube	102mm	58mm	58mm
Length of Tube	2000mm	1800mm	1800mm
Gross Area	1.99m ²	2.34m ²	2.34m ²

3.1.4 Test Method

The thermal performance of solar collector had been performed according to the Chinese National Standard GB/T 4271^[1] and EN 12975-2^[2]. Before testing, the collector should be pretreated and the cover plate, vacuum tube, and reflector should be thoroughly cleaned. During formal testing, maintain the set operating conditions. During the steady-state testing phase, each operating condition must maintain a stable flow rate (deviation $\leq \pm 5\%$), total irradiance ($\pm 50\text{W/m}^2$), ambient temperature ($\pm 1.5\text{ }^\circ\text{C}$), working fluid inlet temperature ($\pm 0.1\text{ }^\circ\text{C}$), working fluid outlet temperature ($\pm 0.4\text{ }^\circ\text{C}$) and other parameter deviations. At least four sets of data should be recorded during the testing.

3.1.5 Test Conditions

There were more than 100 sets of solar collectors tested in a year, so tests were started and finished on different days.

The aging test for different solar collectors started and finished at different times. Detailed test conditions are listed in Table 3.

Table 3: Test Conditions.

Solar Collector	FPC	GSETC	HPETC	UETC
Started Day	12 th , Jul.	6 th , Jun.	14 th , Apr.	26 th , Feb.
Finished Day	8 th , Oct.	27 th , Oct	12 th , Sep.	24 th , Oct
Total Irradiation on The Aperture (MJ/m²)	1170	1887	1404	1954
Average Ambient Temperature (°C)	25.2	24.2	26.7	24.3
Duration (day)	88	143	151	241



Daily Irradiation (MJ/m ²)	13.6	13.2	9.3	8.1
--	------	------	-----	-----

3.1.6 Thermal Performance Test Result

After aging test, the thermal performance of solar collectors was all lower, the curve before and after test are listed in Table 4, Figure 3 to Figure 6.

Table 4: Thermal Performance Before and After Test (Based on Inlet Temperature, Aperture Area).

	FPC	GSETC	HPETC	UETC
Before Test	$\eta_a=0.769-5.055T_i^*$	$\eta_a=0.752-2.462T_i^*$	$\eta_a=0.768-2.361T_i^*$	$\eta_a=0.738-2.444T_i^*$
After Test	$\eta_a=0.658-7.669T_i^*$	$\eta_a=0.737-4.015T_i^*$	$\eta_a=0.694-7.910T_i^*$	$\eta_a=0.620-6.438T_i^*$

Table 4 and Figure 4-7 show all efficiency ($T_i^*=0$) (curve intercept) dropped down, and all heat loss coefficients of solar collectors were increased after aging test.

In Chinese National Standard, requirement for thermal performance of flat plate collector is $\eta_a=0.72 - 6.0T_i^*$, for evacuated solar collector is $\eta_a =0.60 - 3.0 T_i^*$. Before test, all the test results could satisfy the requirements. After test, all the index, especially the heat loss coefficient, were lower, and the performance could not meet the requirements of Chinese national standard.

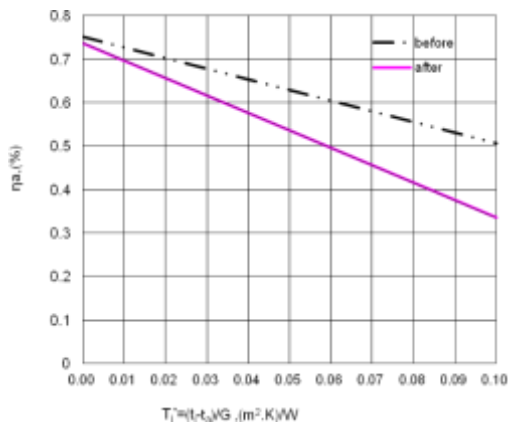


Figure 4: Thermal Performance Change of FPC.

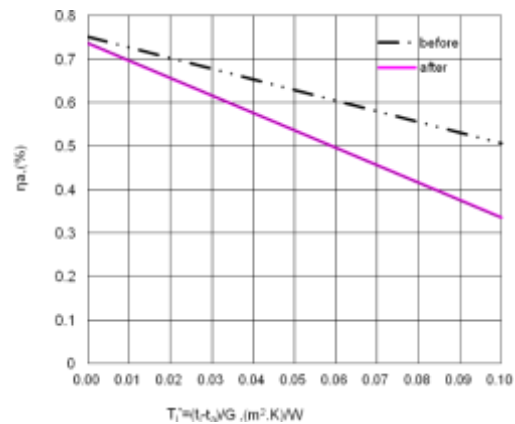


Figure 5: Thermal Performance Change of GSETC.

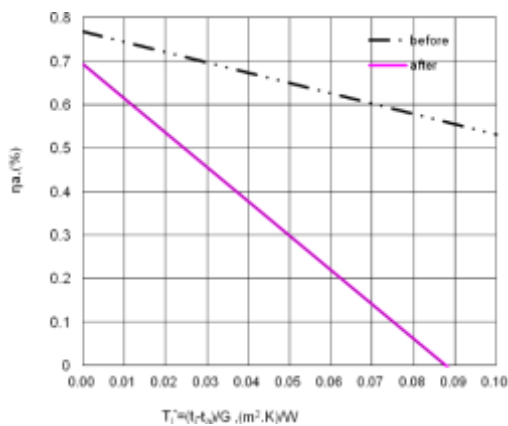


Figure 6: Thermal Performance Change of HPETC.

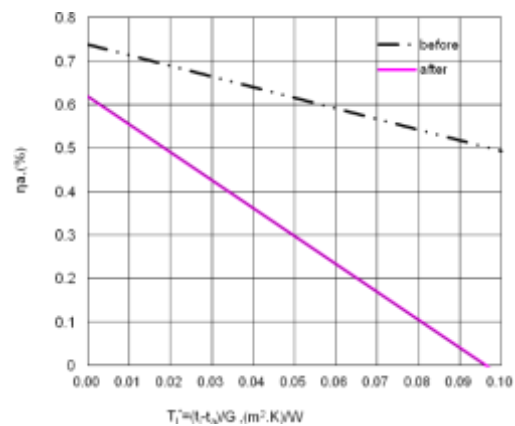


Figure 7: Thermal Performance Change of UETC.

3.1.7 Conclusion

From the aging test result, we can draw a conclusion that the thermal performance of solar collectors was reduced after aging test.

For ETCs, the optical efficiency ($T_i^*=0$) (curve intercept) dropped little. However, all the heat loss coefficients increased. In the case of X, the heat loss coefficients of GSETC increased from 2.462 to 4.015, a massive 63.1% increase. For the HPETC, the heat loss coefficients increased from 2.361 to 7.910, 235% increase. For the UETC, the increase was from 2.444 to 4.438, which represents an 81.6% increase. Compared with FPC, the aging test has more significant effect on the performance of ETCs. The possible reason could be that the insulation material, such as the rubber ring, has more influence on thermal performance.

3.2 Overheating Control

3.2.1 Introduction

Overheating represents a critical operational challenge in pressurized thermosyphon solar water heaters employing all-glass evacuated tubes with integrated heat pipes, particularly during stagnation conditions when hot water remains unconsumed. Prolonged exposure to stagnation temperatures exceeding 150°C accelerates material degradation, promotes thermal decomposition of working fluids, compromises seal integrity, and shortens system lifespan.

Currently, addressing overheating issues in siphon-type solar water heaters primarily relies on three technical approaches: First, promptly releasing excess heat through heat dissipation and pressure relief devices (such as T/P safety valves or anti-overheating sealed tubes). Second, employing smart shading collector tubes or automatic sunshade mechanisms to block sunlight collection during high temperatures. Third, enhancing heat collection efficiency by optimizing system circulation structures and applying high-temperature, low-efficiency absorber coatings. These methods collectively balance system efficiency with overheating risks, providing users with solutions that prioritize both safety and durability.

However, conventional mitigation approaches—such as physical shading, auxiliary ventilation, or passive heat dissipation—often incur significant efficiency penalties or introduce operational complexities, failing to balance performance with reliability. Mert Çimen et al. have proposed an innovative overheating restriction strategy based on precise adjustment of the working fluid inventory in heat pipes^[1].

The specific research methods and results are as follows:

3.2.2 Main Research

3.2.2.1 Experimental Design and Methodology

The study employed a controlled solar simulator to evaluate the performance of all-glass evacuated tubes (AGETs) under reproducible conditions, eliminating weather-related variability. Tests were conducted at two distinct temperature environments (16–18°C and 40°C) to simulate moderate and high-ambient conditions. Key performance metrics included startup behavior, water temperature rise kinetics, and stagnation characteristics. AGETs were filled with three working fluids—ethanol, methanol, and acetone—at volumes calibrated to achieve a theoretical maximum operating temperature of 80°C. Field validation was concurrently performed using a standard 24-tube thermosyphon system under real environmental conditions, with continuous monitoring of tank temperature, ambient conditions, and solar irradiance, as shown in Figure 8.



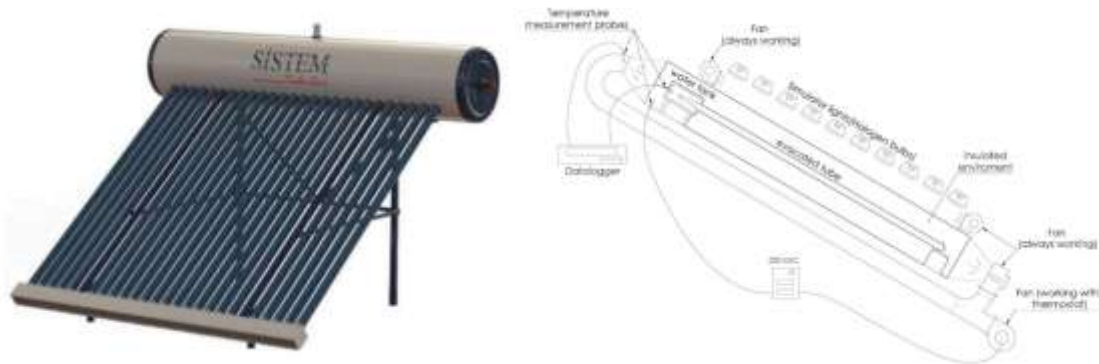


Figure 8: Ephesus Thermosyphon Solar Water Heater with 24 AGETs and Schematic Diagram of The Solar Simulator Set Up for The Conditioned Medium Used in The Field Experiments.

3.2.2.2 Performance Analysis and Fluid Comparison

Ethanol demonstrated superior performance characteristics under both simulated and field conditions. In controlled tests, AGETs with 4 ml ethanol exhibited near-linear temperature rise to 75°C before efficiency attenuation mitigated stagnation risks. Comparative analysis revealed ethanol's optimal balance between operational efficiency and thermal regulation, while methanol and acetone showed suboptimal heat transfer stability at elevated temperatures. Under 40°C environment simulations, ethanol-based systems maintained predictable temperature stabilization at 95°C during simulated stagnation, leveraging inherent thermophysical properties to reduce heat transfer efficiency above 80°C.

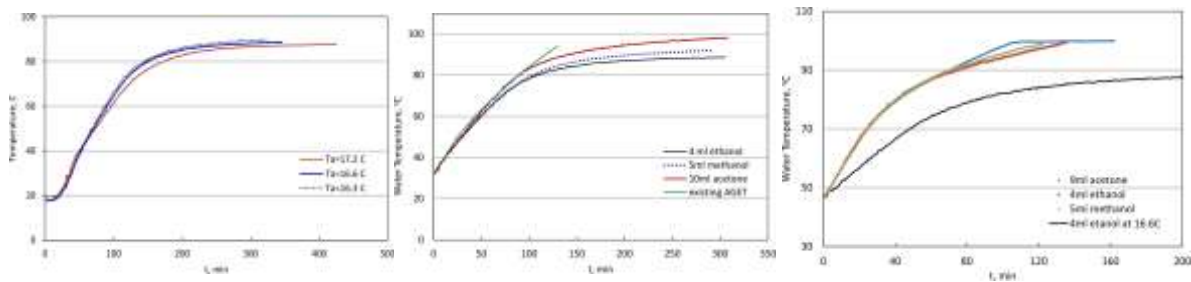


Figure 9: Solar Simulator Test Results.

3.2.2.3 Efficiency and Validation

Solar thermal conversion efficiencies were quantified against the solar thermal condition. Ethanol-filled AGETs achieved 77.5% daily conversion efficiency (aperture-based) at 80°C operation during field trials, aligning closely with simulator data. Although initial field performance matched conventional systems, efficiency divergence occurred over subsequent days due to engineered thermal regulation mechanisms. This deliberate efficiency reduction above 80°C enables critical overheating protection without compromising baseline performance. The synthesis of operational efficiency, cost-effectiveness, and fluid stability confirmed ethanol as the optimal working fluid, leading to its commercial adoption in pressurized thermosyphon systems.

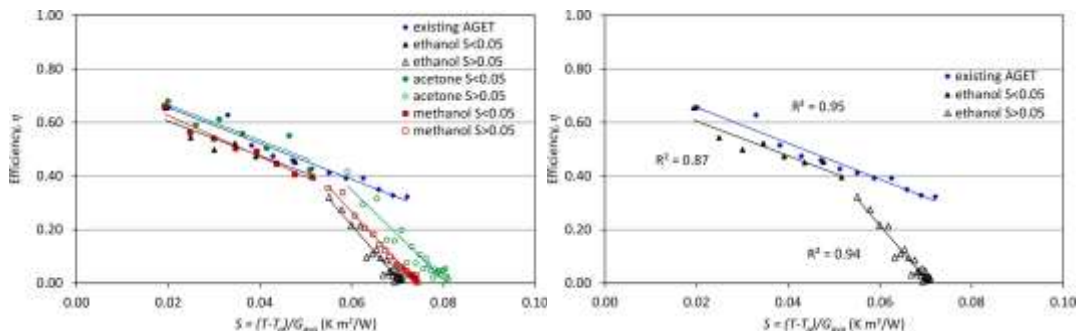


Figure 10: Solar Heating Efficiencies.

3.2.2.4 Implications for System Durability

The research demonstrates that controlled working fluid inventory management directly addresses the fundamental trade-off between efficiency and overheating. By exploiting the dry-out limit phenomenon, ethanol-filled AGETs achieve self-regulating thermal behavior without auxiliary controls. This paradigm enhances system longevity by reducing thermal stress on materials and seals during stagnation, while maintaining competitive efficiency during normal operation. The experimental framework establishes a replicable methodology for validating overheating mitigation strategies in solar thermal applications.

3.2.2.5 Conclusion

This study establishes that controlled overheating mitigation through heat pipe working fluid regulation represents a transformative approach to enhancing the durability and reliability of all-glass evacuated tube (AGET) thermosyphon systems. The experimental results demonstrate that precise management of ethanol inventory—specifically utilizing a 4 ml filling volume—creates a self-regulating thermal mechanism that effectively caps stagnation temperatures at 95°C while maintaining conventional efficiency levels up to 80°C. This is achieved through intentional operation near the dry-out limit, where heat transfer efficiency deliberately decreases as system temperature approaches critical thresholds, thereby providing inherent protection against extreme thermal stress without requiring active interventions or sacrificing performance under normal operating conditions.

The selection of ethanol as the optimal working fluid is validated through comprehensive comparative testing under both simulated and environmental conditions. Its superior thermal properties enable a daily conversion efficiency of 77.5% while simultaneously providing predictable overheating protection—a critical dual capability that methanol and acetone failed to deliver with equivalent consistency. The research confirms that this approach directly addresses the primary failure modes associated with overheating: material degradation, seal failure, and working fluid decomposition. By maintaining peak temperatures below destructive thresholds, the system significantly reduces thermal cycling stress on glass-to-metal seals and prevents polymer component failure, thereby extending functional service life.

Furthermore, this research provides both a methodological framework for evaluating overheating mitigation strategies and a proven technical solution that balances performance preservation with durability enhancement. The findings offer manufacturers a cost-effective, reliability-driven approach to product improvement that addresses one of the most persistent challenges in solar thermal technology deployment across variable climate conditions.

3.2.3 Development Direction

Future siphon-based solar anti-overheating technology will evolve toward intelligent, passive, and systematic coordination. Key developments include:

- AI-driven control systems based on weather forecasting.
- Application of self-shading and phase-change thermal storage materials requiring no external power.
- Integrated photovoltaic-solar thermal designs for energy conversion.

These innovations aim to shift from “passive response” to “proactive prevention,” establishing safer and more efficient thermal management systems.

3.3 Mitigate Heat Loss

3.3.1 Introduction

Nighttime heat loss has always been an unfavorable factor affecting the operating efficiency and reliability of solar water heating systems. Addressing heat loss in siphon-type solar water heaters primarily relies on three technical approaches: optimizing vacuum tube structures and selective absorption coatings to significantly reduce radiative heat loss; thickening polyurethane insulation layers and employing seamless encapsulation techniques to effectively suppress conductive heat loss; and implementing intelligent temperature-controlled circulation systems that automatically start and stop circulation pumps during low-temperature periods, thereby minimizing heat loss during non-usage intervals.



In addition to this, Sami Awani et al proposed a new design of a solar thermosyphon water heating system with phase change material and tested the design using experimental and numerical simulation methods. The experimental results prove that the design does indeed have this function^[2].

The specific research methods and results are as follows:

3.3.2 Main Research

3.3.2.1 Experimental Scenario Setup

The system consists of a horizontal cylinder serving as the storage tank and a conventional flat plate solar collector.

The external wall of the newly proposed tank is made of glass to ensure the maximum absorption of solar radiation during the day. The internal wall is made of metal to have good conductivity with the water inside the tank. A PCM (paraffin) is inserted between the external and internal walls to conserve the stored heat as shown in Figure 11. The specifications of the used tank listed in Table 5.

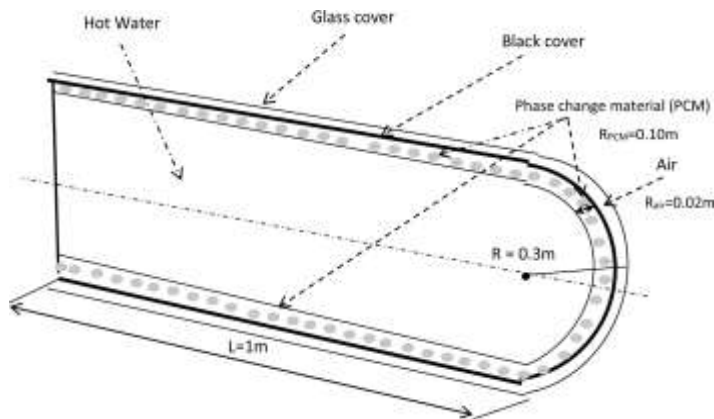


Figure 11: Longitudinal Division of New Storage Tank.

Table 5: Specifications of Thermal Storage Tank.

Item	Specification
Thermal Conductivity	1.5 (kJ.hr ⁻¹ .m ⁻¹ .k ⁻¹)
Tank Configuration	Horizontal Cylinder
Overall Loss Coefficient	5 kJ.hr ⁻¹ .k ⁻¹
Initial Temperature	20 °C
Volume	280 l

The geographical location of the experiment is on the north of Tunisia, which lies in the sunbelt with high solar irradiance. For determining the thermal performance of the heating system, simulations and experiments were conducted during three days in different seasonal conditions on the first day of January, March, and July. The solar radiation conditions during the experiment are shown in Figure 12.

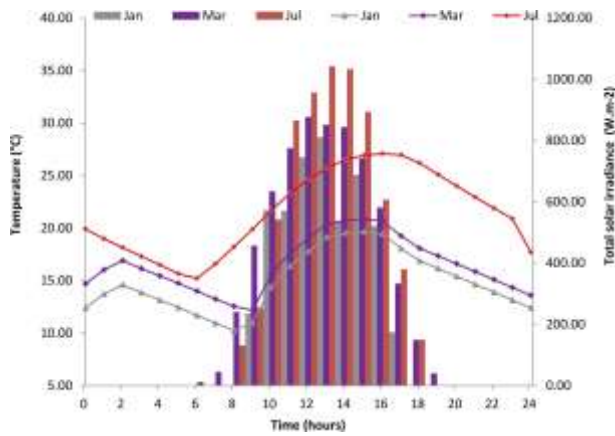


Figure 12: Total Solar Irradiance on The Surface of Thermosyphon and Ambient Temperature for A Particular Day 1st of January, March, and July.

3.3.2.2 Results of Experimental

To verify the superiority of the newly designed system over the traditional system, this experiment will compare the tank with PCM and the classic one. Figure 13 shows the temperature of the water flowing into the storage tank.

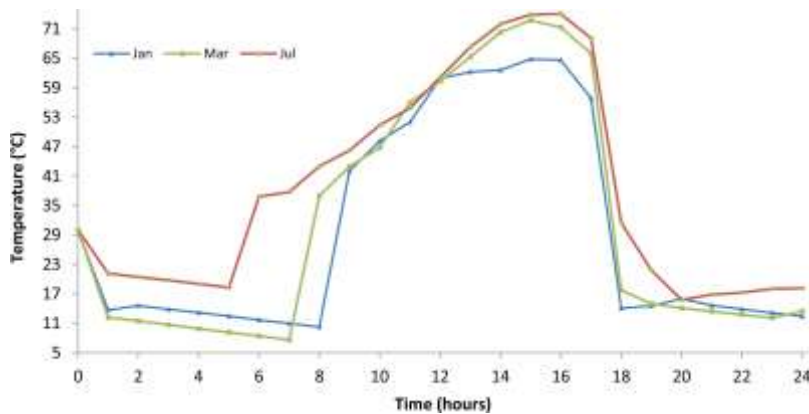


Figure 13: Temperature Variation of The Water Flowing into The Storage Tank from The Collector for A Particular Day (1st of January, March, and July).

Figure 14 shows the variation of the water tank temperature inside of the classic case as a function of daytime. A noticeable drop in temperature can be observed at night. This decrease is due to thermal losses of the reservoir during the night. Therefore, this signifies that the thermal insulation of the classic tank is insufficient to avoid thermal losses during the off-sunshine hours.

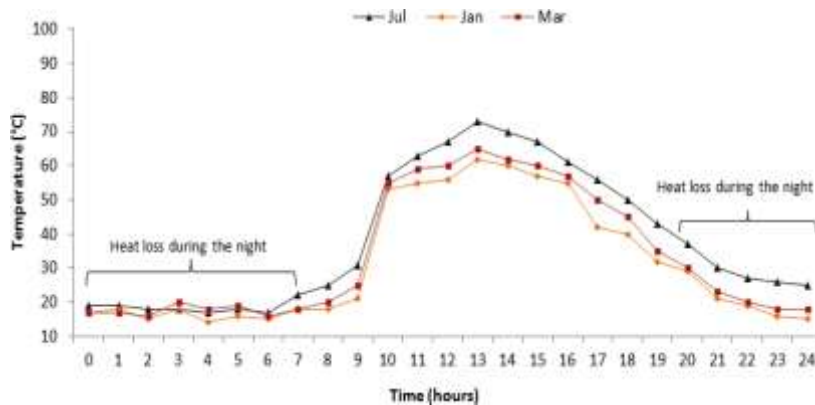


Figure 14: Variation of Water Temperature inside The Classic Tank.

The charging phase starts from 9:00 am to 4:00 pm. During this period, the temperature gradually rises above the melting point as shown in Figure 15, and the PCM layer of the tank receives solar radiation and solar energy is stored in sensible and latent heat forms.

To maintain the highest water temperature inside the tank during the night (off-sunshine hours), the PCM changes from the liquid to the solid state and liberates the stored heat. See Figure 16 for temperature changes.

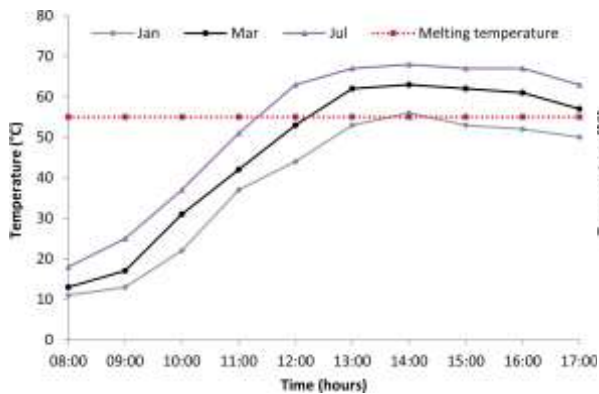


Figure 15: Experimental Temperature Variation of The Phase Change Material in The Charging Phase.

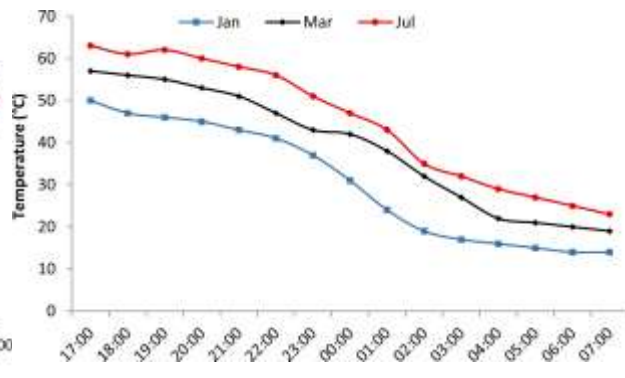


Figure 16: Experimental Temperature Variation of the Phase Change Material in The Discharging Phase.

To more clearly demonstrate the performance differences between the new and old storage tanks, the two designs of the storage tank in July and January are shown in Figure 17.

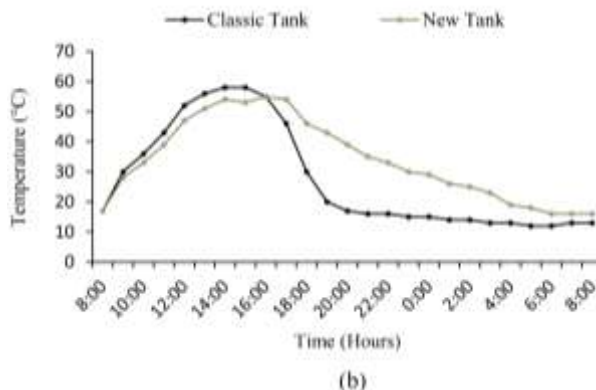
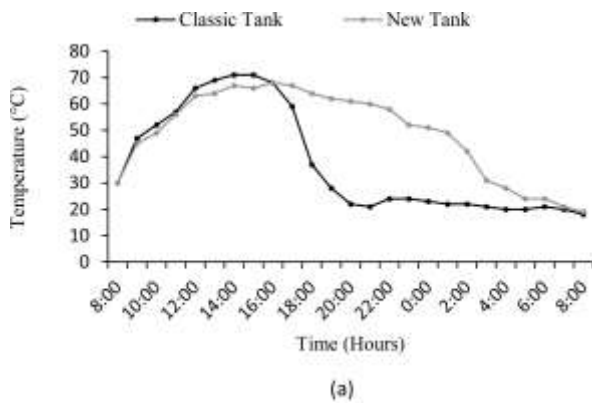


Figure 17: Temperature Variation of Water inside The New and Classic Thermosyphon Tanks on A (a) Summer Day (b) Winter Day.

In this experiment, TRNSYS was used to build a model of a PCM phase change storage tank. The accuracy of the model was verified based on experimental and already published data. The verification results are shown in Figure 18. An error of less than 4% for the tests in summer and winter.

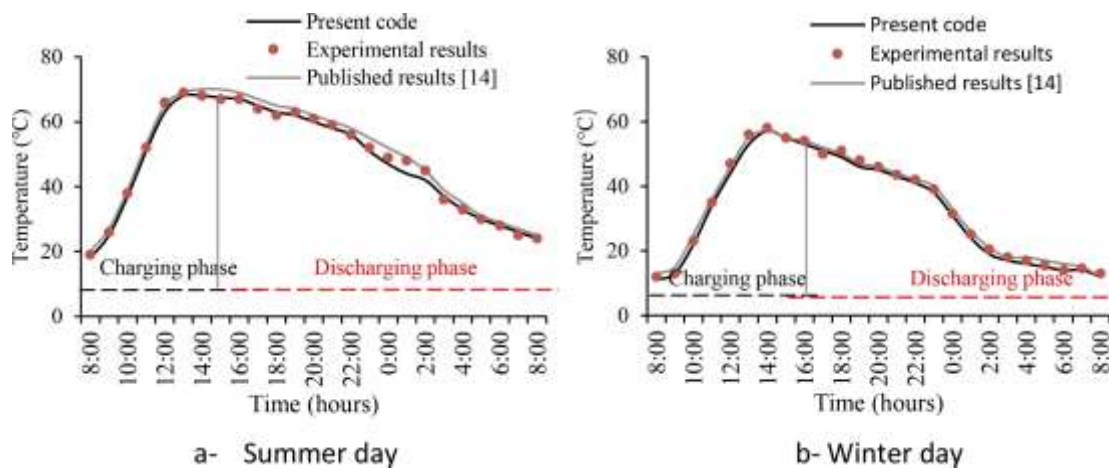


Figure 18: The Comparison of The Current Results with Experimental and Published Data on A (a) Summer Day and (b) Winter Day.

Modelling approaches were adopted in the present to model the thermal behaviour of the PCM with a CFD code. Thermal fields in the charging and discharging phase are shown in Figure 19 and 20.

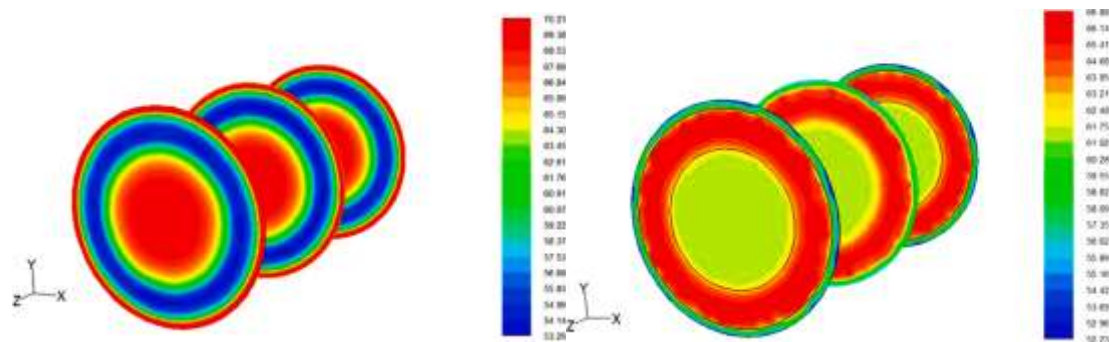


Figure 19: Thermal Fields in The Charging Phase. Figure 20: Thermal Fields in Discharging Phase.

3.3.2.3 Conclusion

The thermal storage tank has a significant impact on the performance of solar thermosyphon water heating systems. Traditional thermal storage tanks are unable to solve the problem of heat loss at night, and the large amount of heat wasted seriously affects the efficiency of the entire system.

The present work investigated numerically and experimentally the thermal performance of a new thermosyphon design of the solar water heating system, which resolved the issue effectively. It was found that the thermosyphon tank design had a significant effect on the system's performance. The durability of hot water availability increased by more than 40% since the phase change material reduces heat losses to the surroundings.

This design solves the core problem of heat loss at night in solar hot water systems through innovative PCM and water tank structures. It is both technically feasible and economically viable.

3.3.3 Development Direction

Future heat loss prevention technologies for siphon solar water heaters will focus on three key areas:

- Developing high-performance insulation materials such as nanoporous composite insulation and vacuum insulated panels to significantly enhance the thermal insulation of tanks and piping.
- Advancing intelligent control systems that utilize multi-sensor networks to monitor environmental parameters and water demand, enabling precise on-demand heating.
- Widespread adoption of phase change thermal storage materials to accumulate excess heat during daylight hours and release it at night, effectively stabilizing temperature fluctuations.

3.4 Freeze Protection

3.4.1 Introduction

Thermosyphon solar water heating systems operate with no pumps or sensors, but in cold climates, water stored in the piping system of siphon-type solar water heaters is prone to freezing at low temperatures. The resulting volume expansion can cause pipes or collectors to burst. Traditional anti-freeze methods (such as using antifreeze or installing pump-controlled systems) are complex and costly, making them difficult to promote.

The primary methods for preventing freezing in siphon-type solar water heaters include drain-and-drain freeze protection, circulating antifreeze, electric trace heating insulation, and improved system design. Among these, draining prevents freezing by automatically emptying pipes of water during low temperatures to avoid ice formation; the antifreeze circulation system utilizes heat exchangers to transfer heat; electric trace heating technology maintains pipe temperatures through temperature-controlled cables, while optimizing circulation structures and employing freeze-resistant materials enhance freeze resistance at the design level.

To address this issue, a thermosyphon driven supercritical CO₂ fluid based solar water heating system is developed for use in subzero temperature areas, which is proposed by N. Abas et al. This innovative solar water heater can perform adequately at subzero temperatures where water-based systems fail to perform well due to freezing^[3]. Robert Stayton proposes a fully passive, external-energy-free anti-freeze design. By adding an additional circulation loop connected to the heat source below the collector, it utilizes density changes caused by water temperature differences to achieve natural circulation, thereby preventing freezing^[4].

The specific research methods and results are as follows:

3.4.2 Main Research: Applications of Supercritical CO₂ Fluids

3.4.2.1 Experimental Scenario Setup

The experiment focused on the thermosyphon driven supercritical fluid based solar water heating system construction and tested system performance, including operational stability, environmental adaptability, and operational energy efficiency.

A solar collector consisting of nine borosilicate evacuated glass tubes fitted on an aluminium stand. Evacuated glass tubes are placed inclined in aluminium stand facing south at a local latitude angle of Islamabad, Pakistan (33 °). A high-pressure CO₂ filling system was developed as part of solar water heating system, is operated by a manual three-way stainless-steel valve.

It should be noted that CO₂ has a higher saturated working pressure than water, so special heat transfer tubes are used, its arrangement is divided into two types: serpentine and parallel. System photos are shown in Figure 21.



Figure 21: Front and Rear View of Solar Water Heating System with CO₂ Filling Circuit.

The experiment site is located at Pakistan. In northern areas of Pakistan like Gilgit-Baltistan (35.8026°N,74.9832°E), the average temperature in winter (-10 °C), chilly winds and local weather conditions are the major hindrances in

the exploration of solar energy. The possible sunshine hours during any typical month remains in the range of \pm 40% with low ambient temperature as shown in Figure 22.

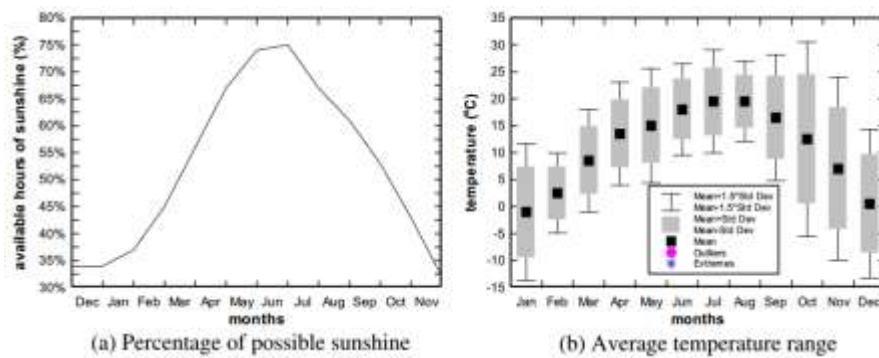


Figure 22: Climate of Gilgit-Baltistan (Pakistan).

3.4.2.2 Results of A CO₂-based Solar Collector

A solar water heating system using CO₂ refrigerant and evacuated glass tube (EGT) collector was tested in winter weather conditions of Islamabad, Pakistan. Serpentine and parallel U tubes experimental arrangements were filled with CO₂ at a pressure of 40 bar for initial testing. The results of sub critical operation are shown in Figure 23.

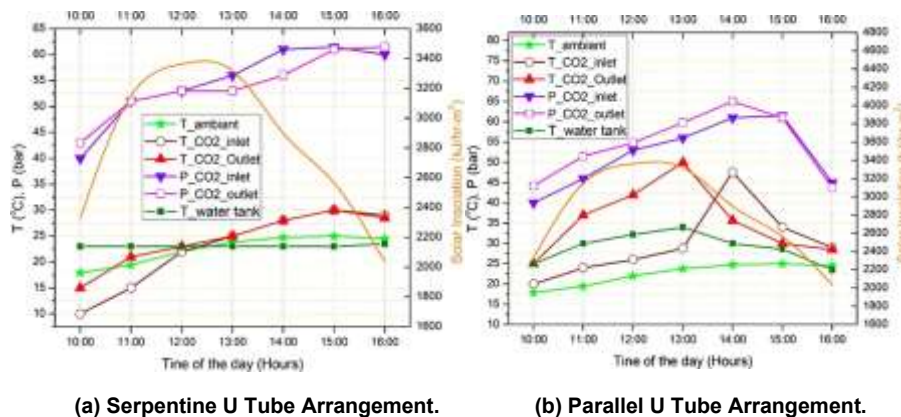


Figure 23: The Result of Serpentine and Parallel U Tube Arrangements in Solar Water Heater.

During the test, thermosyphon phenomena were not observed in serpentine U tube setup. This may be attributed due to internal cancellation of thermosyphon effect in series connected U-tubes. Serpentine arrangements require a CO₂ pump to circulate the heat carrying fluid pump to circulate the heat carrying fluid.

Contrary to serpentine scheme, in parallel U-tube setup, the heat transfer between source and sink proceed smoothly. However, due to cloudy weather and a reverse thermosyphon was noted in parallel U tube setup. The non-return valve (NRV) originally used to stop the reverse flow of CO₂ in mild sunshine or cloudy conditions in temperature climate was blocked and caused a permanent blockage in the system loop as shown in Figure 24.



Figure 24: Blockage of NRV Due to Dry Ice CO₂.

A modified solar collector consisting of nine EGT and a set of nine U shape heat removal copper tubes, as shown in Figure 25. The Hot header was placed at higher datum level as compared to cold header. The hot header was inclined upward an angle more than 20° to stop reverse thermosyphon. This modification increased the height of water tank was increased and a tilt angle of 45° was introduced in up riser for the same purpose. The downcomer was trailed a bit downward to ensure one-directional flow from hot header to the water tank and then back to the collector.



Figure 25: Innovative Design of Manifold with U Shaped Copper Tubes.

Figure 26 shows solar insolation and ambient temperature plot versus the time during a typical sunny day during winter season in Pakistan. The useful heat gain and solar collector efficiency of improved system as shown in Figure 27. Figure 28 shows the results of same parallel U tube configurations during a mild-sunny day when the average ‘ambient temperature remains below 20 °C.

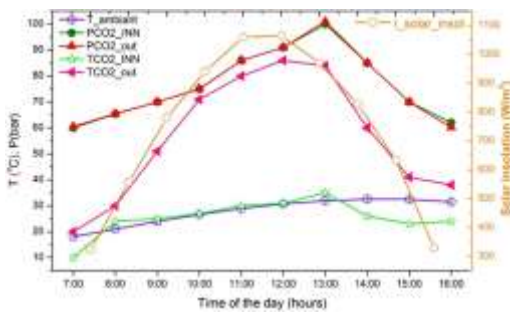


Figure 26: Variation of Collector Output Temperature and Pressure from 7 AM to 16 PM.

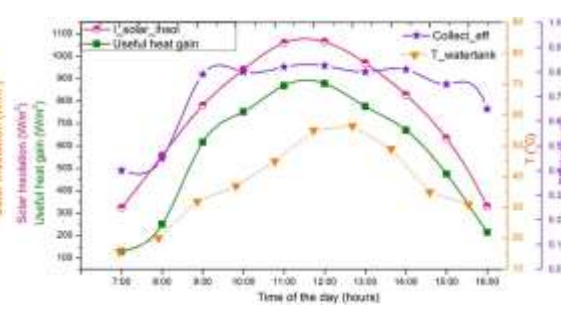


Figure 27: Useful Heat Gain and Efficiency of System.

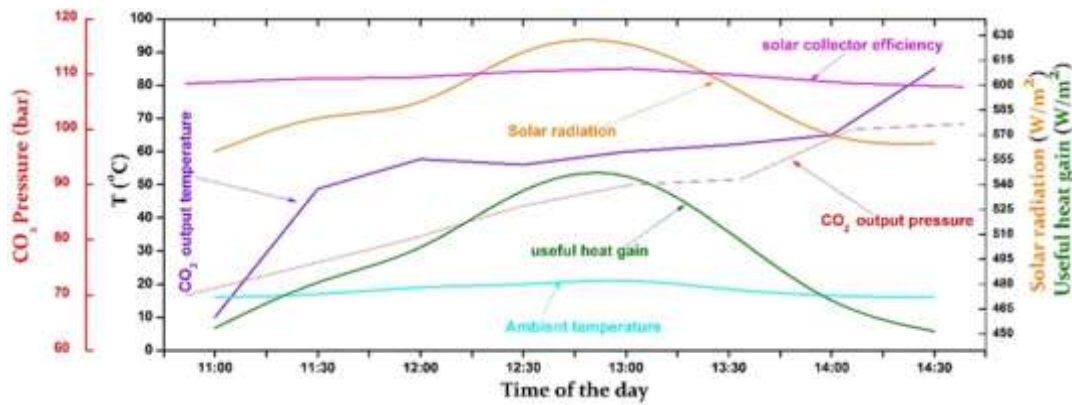


Figure 28: Performance of Solar Water Heating System During a Mild Sunny Day.

3.4.2.3 Conclusion

The results indicated that the system can still run smoothly in cold environments and is efficient and technically feasible. Moreover, newly design thermosyphon solar water heating system showed a solar collector efficiency of 85% with a net useful heat gain of 71% even in mild sunshine.

This work combines supercritical CO₂ with thermal siphon vacuum tube collectors for the first time, overcoming the technical bottleneck of solar hot water systems in severely cold regions and providing an innovative solution for the application of renewable energy in extreme environments.

3.4.3 Main Research: Passive Freeze Protection

3.4.3.1 Principle of Operation

The Dual Loop Passive Freeze Protection utilizes the principle that cold water sinks because it is denser. Based on this principle, this solution adds a second water circulation loop that connects to a heat source below the collector. The extra loop is added using simple pipe T fittings.

One T fitting is added to the plumbing at the bottom of the collector, a second T fitting is added to the plumbing at the top of the collector, and direct plumbing is used between the T fittings and the heat source mounted below the collector. No check valves or pumps are used because the second loop is self-powered and self-regulating, like the upper heating loop.

The Dual Loop Thermosyphon can be seen in Figure 28, and Figure 29 depicts a classic cycle to illustrate the differences.

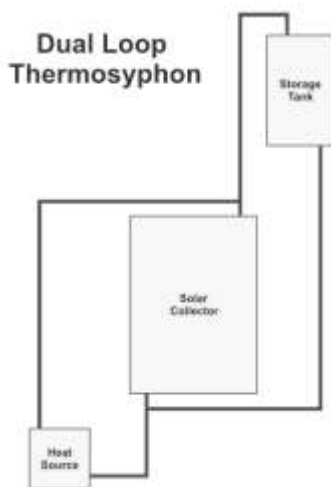


Figure 29: Dual Loop Thermosyphon.



Figure 30: Classic Thermosyphon.

This arrangement operates as follows. During the day, the upper loop is active, and the system operates as a classic thermosyphon system, as shown in Figure 31. At night, when the temperature in the collector drops, the lower loop is activated, as shown in Figure 32.

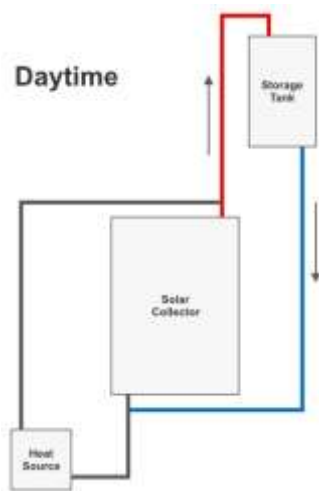


Figure 31: Daytime Operation.

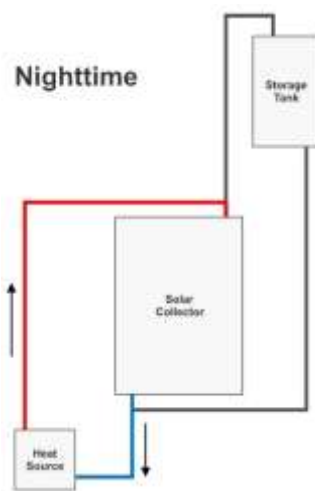


Figure 32: Nighttime Operation.

The heat source below the collector does not have to be very hot; it just must keep the water temperature above the maximum density of water at 4°C (39°F).

Providing a heat source for such mild temperatures is easy. Potential sources include the following:

- Ambient heat from a building interior absorbed through a heat exchanger.
- Ground heat from a buried coil.
- Active heater with a thermostat (no longer passive, however).

The two water loops have little crossover because of the overall temperature stratification in the system. If the heat source below the collector is cooler than the water stored in the tank, then the upper loop will not be activated at night. Likewise, during the day, the lower loop will not be activated unless the cold water from the tank is colder than the lower heat source.

3.4.3.2 Demonstration System

To validate the effectiveness of this method in actual operation, A demonstration system was built in 1999 and has successfully operated since then.

The full-size demonstration system is in Santa Cruz in Northern California, an area that typically experiences several freezing nights per year, reaching temperatures as low as -7°C (20°F). The solar collectors are mounted on a hillside and are shown in Figure 33.

The warm water exits at the top of the collectors and is carried in a one-inch copper pipe that is wrapped in insulation and buried in a trench to convey the water to the 100-gallon storage tank in the house. A second one-inch copper pipe returns cold water from the bottom of the tank to the bottom of the collectors. See Figure 34. The freeze-protection loop is buried in a trench below the collectors and connects to a coil of copper tubing buried in the ground, as shown in Figure 35.



Figure 33. Solar Collectors.



Figure 34. Classic Thermosyphon Pipes above The Collectors.



Figure 35. Lower Loop Connects to Buried Coil.

The coil is buried three feet deep where the soil never reaches freezing temperatures. At night, the coil absorbs heat from the ground to keep it above freezing temperatures. When the collector's water temperature drops below the ground temperature, the lower circulation loop starts up and delivers sufficient heat from the soil to the collectors to prevent them from freezing.

This system has provided a reliable supply of hot water on sunny days. During the 20+ years of operation, no pipes have ever frozen and burst, despite temperatures recorded on the surface of the collectors as low as -7°C (20°F). Other standing water near the collectors did freeze on such nights. The system has operated all those years with zero maintenance, other than occasionally washing the collector glass.

3.4.3.3 Conclusion

The exemplary project's sound condition proves that the dual-loop passive freeze protection design proposed in this paper offers a simple, reliable, and low-cost solution that effectively expands the climatic applicability of thermosyphon solar water heating systems.

This system requires no external power source and no maintenance, making it suitable for DIY projects, developing countries, remote areas, and similar scenarios. Additionally, by utilizing heat sources underground or within buildings, frost protection can be achieved without adding complex equipment, offering high practical value and significant potential for widespread adoption.

3.4.4 Development Direction

The development directions for siphon-type solar freeze protection technology are as follows:

- Integrating smart control, the system automatically drains residual water from pipes via temperature sensors and resumes water supply once temperatures rise.

- Improving heat transfer media by using specialized antifreeze fluids that maintain fluidity at extremely low temperatures for heat transfer.
- Optimized piping design and insulation employ non-trapping elbow configurations, paired with high-performance insulation materials and self-regulating electric heating cables to maintain pipe temperatures.

These approaches effectively resolve freezing issues across diverse climatic conditions through the integration of intelligent control and system design.

3.5 Loop Thermosyphon Technology

3.5.1 Introduction

Loop thermosyphon (LT) is usually introduced to overcome the freezing and corrosion problems associated with the conventional solar water heating (SWH) system. Loop siphon solar water heaters have secured a place in residential hot water supply due to their pump-free operation and quiet, reliable performance. Current research is focused on enhancing their efficiency and stability across diverse environmental conditions.

To compare its difference between the LT-SWH system and the conventional SWH system, T. Zhang et al. conducted experiments based on the typical meteorological year data of Fuzhou city to analyze annual performances of above two systems, including the effective number of supplying days, effective heat gain and nighttime heat loss^[5].

The specific research methods and results are as follows:

3.5.2 Main Research

3.5.2.1 Experimental Scenario Setup

This study uses a combination of mathematical model simulation and experimental verification to compare and analyze the annual performance of the LT-SWH system and the conventional SWH system under two different operating modes (continuous heating mode and the discontinuous heating mode). Schematic diagrams of the LT-SWH system and the conventional SWH system can be found in Figure 36.

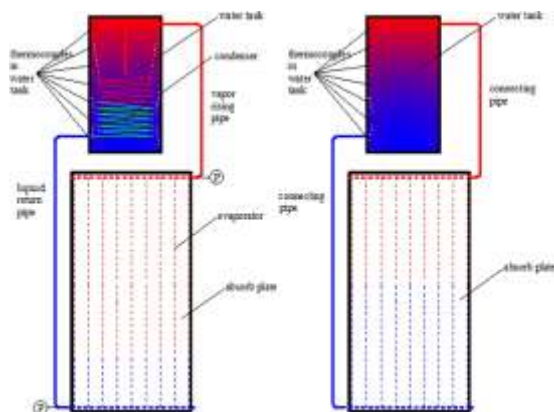


Figure 36: Schematic Diagrams of LT-SWH System and Conventional SWH System.

The experiment was conducted in Fuzhou, which is the provincial capital of Fujian province in China, belongs to the subtropical zone enjoying a humid monsoon climate. Figure 37 illustrates the average monthly direct radiation ratio, the monthly average ambient temperature in Fuzhou city, as well as the monthly cumulative solar radiation projecting on the horizontal plane and the inclined plane.

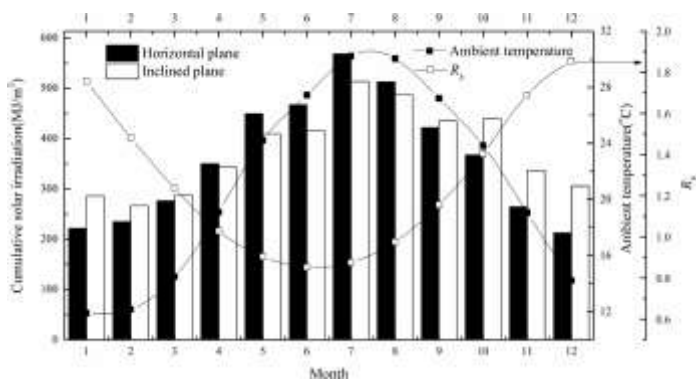


Figure 37: Variations in Monthly Average Ambient Temperature, R_b , Monthly Cumulative Solar Radiation.

3.5.2.2 Experimental Results and Comparison

When only solar energy is used, the monthly effective number of supplying days of the SWH system and the LT-SWH system, under different heating modes, are presented in Figure 38. Under different heating modes, the effective heat gains are illustrated in Figure 39 in detail.

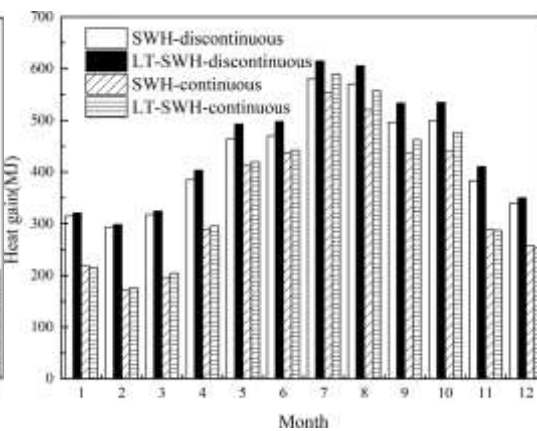
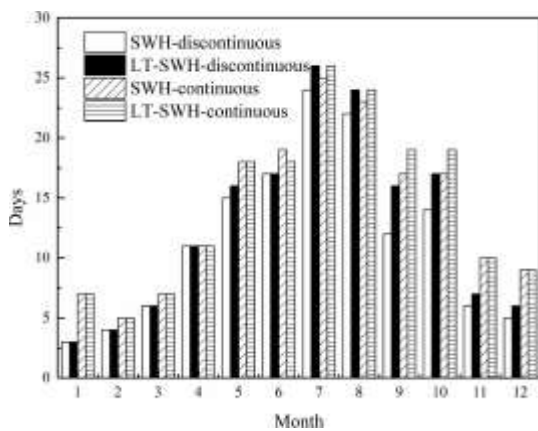


Figure 38: Comparison of The Monthly Effective Numbers under Different Heating Modes.

Figure 39: Comparison of The Monthly Effective Heat Gains of Supplying Days under Different Heating Modes.

It has been calculated that, under the discontinuous and continuous heating modes, the annual effective numbers of supplying days for the SWH system are 139 and 168, respectively; while for the LT-SWH system, they are 153 and 173, respectively.

Figure 39 shows that under the discontinuous heating mode, the effective heat gain of the SWH system is always smaller than that of the LT-SWH system corresponding to the same month. However, under the continuous heating mode, from November to April, the effective heat gain of the SWH system is approximate to that of the LT-SWH system corresponding to the same month; Nevertheless, under the other months, the relative magnitudes of the effective heat gain between two system share the similar trend with the discontinuous heating mode.

The specific values of the monthly cumulative heat loss under different heating modes, as well as the average monthly temperature drops at night, are displayed in Figure 40. The heat loss ratios, which are defined as the heat loss at night to the heat collection in the day, are presented in Figure 41.



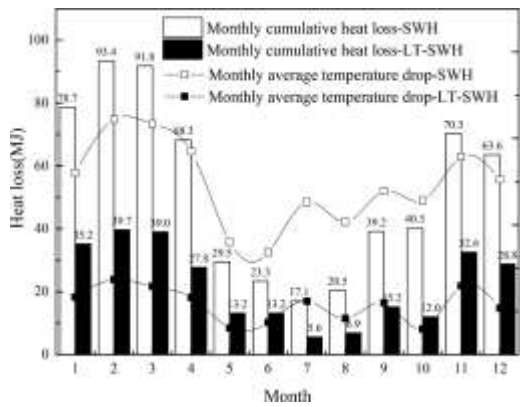


Figure 40: Comparison of Monthly Cumulative Heat Loss and Monthly Average Temperature Drops.

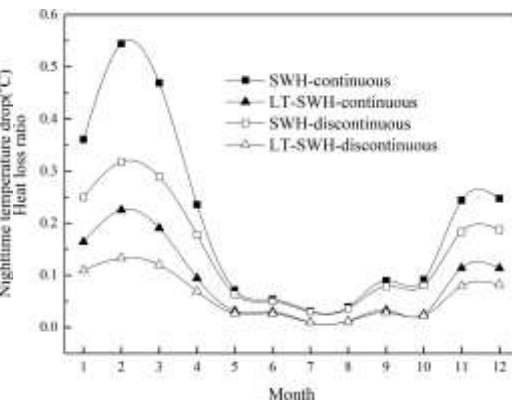


Figure 41: Comparison of Heat Loss Ratios under Different Heating Modes.

From Figure 40 and Figure 41, one can further conclude that under the continuous heating mode, the nighttime heat loss of the SWH system is at least two times that of the LT-SWH system.

The average monthly photothermal efficiencies of the SWH system and the LT-SWH system under different heating modes are shown in Figure 42.

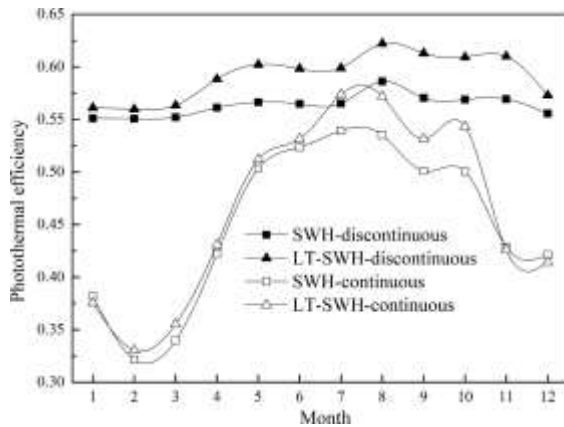


Figure 42: Comparison of Monthly Average Thermal Efficiencies under Different Heating Modes.

It indicates that firstly, the monthly photothermal efficiency of the LT-SWH system is higher than that of the SWH system corresponding to the same month under the discontinuous heating mode.

By calculation, under the continuous heating mode, the annual photothermal efficiency of the SWH system is 46.62%, while it is 48.37% for the LT-SWH system; under the discontinuous heating mode, the values are 56.52% and 59.53%, respectively.

As the set temperature gradually increases, the changes in the performance indicators of the LT-SWH system and the SWH system, and the differences between the two systems are shown in the Figure below.

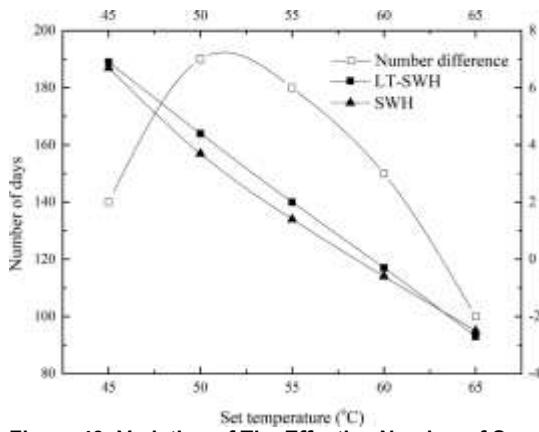


Figure 43: Variation of The Effective Number of Supplying Days with Final Water Temperature.

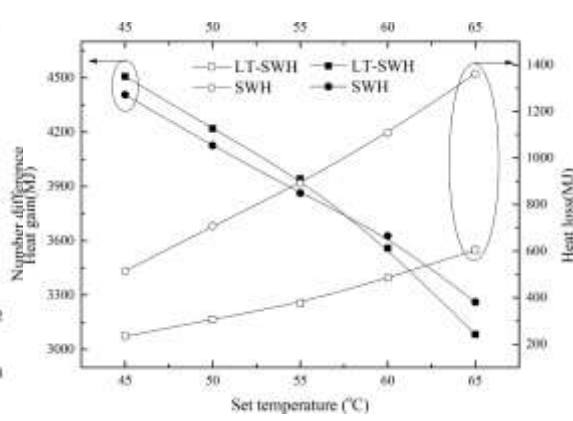


Figure 44: Variation of The Annual Cumulative Heat Gain and Temperature Drop with The Increasing Set.

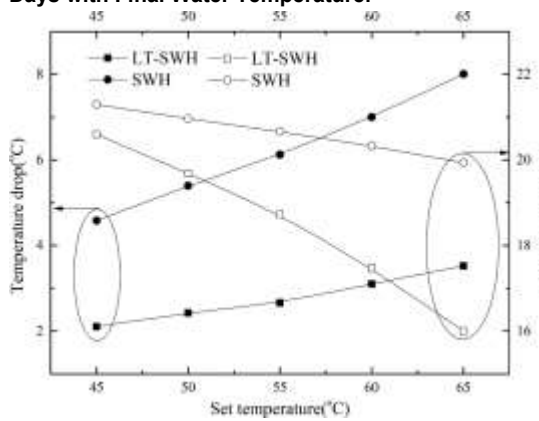


Figure 45: Variations of The Average Annual Temperature Rise, and Temperature Drop with The Increasing Set Temperature.

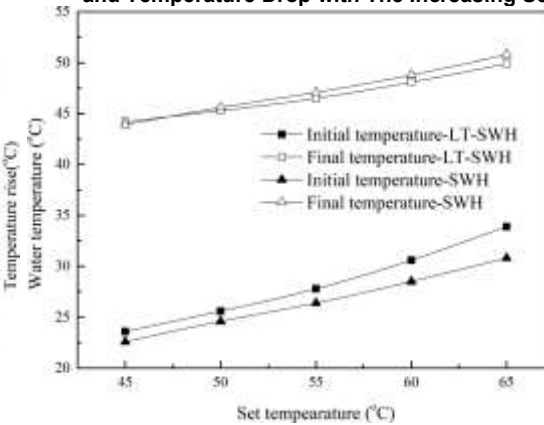


Figure 46: Variations of The Average Annual Initial Water Temperature and Final Water Temperature with Increasing Set Temperature.

For the LT-SWH system, the decisive advantage of the lower heat loss at night gradually fades away and the bigger daytime heat loss gradually begins to dominate the dominance with increasing the set temperature. In addition, the effective heat gain of the LT-SWH begins to be smaller than that of the SWH system when the final water temperature is no less than 60 °C.

3.5.2.3 Conclusion

Integrating loop thermosyphon with a SWH system, named LT-SWH, can avoid the freezing and corrosion problems by tendentiously filtrating of the refrigerant. Also, thermal diode property of loop thermosyphon avoids the reverse flow of heat from water tank to solar collector, which is advantageous to reduce the nighttime heat loss.

In summary, loop thermal siphoning (LT) is an effective technology for improving the durability and reliability of traditional solar water heating (SWH) systems. However, despite the LT-SWH system operating free of corrosion and freezing problems, it is conditional to substitute with the conventional SWH system, especially when the water temperature on demand is high.

3.5.3 Development Direction

Loop siphon solar water heaters are evolving toward greater efficiency, intelligence, and integration. Research focuses on enhancing system thermal performance and reliability, including the application of novel selective absorber coatings, integration of phase change thermal storage materials to reduce heat loss, and adoption of heat transfer enhancement structures such as microchannels. In intelligent control, multi-sensor networks and machine learning algorithms enable system condition monitoring and predictive maintenance, making operation management more precise and efficient. Concurrently, system architecture and heat transfer fluids undergo continuous optimization, with a growing trend toward deep integration with building energy systems. This includes developing photovoltaic-thermal integration technologies, propelling the evolution from standalone water heating equipment to a vital component of comprehensive building energy systems.

4 Technical Solutions

After analyzing research on enhancing the reliability and durability of solar energy systems, the following section will discuss practical solutions ranging from structural design to intelligent operation and maintenance. These solutions go beyond theoretical exploration, focusing instead on specific technical pathways in engineering practice to provide actionable implementation strategies for improving system longevity.

4.1 Technical Solutions for Component Installation and Fixation

4.1.1 Anti-Vibration Support System Design

The long-term stable operation of thermosyphon systems relies on scientifically designed supports. Here are some relevant technologies that can address this issue.

- The main frame incorporates a sliding mechanism and mechanical trigger system. When the system detects high-frequency vibrations caused by strong winds, it automatically triggers locking or stress-relief actions to protect core components^[6].
- For continuous vibrations generated by internal equipment such as water pumps, composite vibration isolation systems can be employed. For instance, rubber bases with upper and lower fluid reservoirs and damping channels can be installed within support feet. The reciprocating flow of fluid within these reservoirs dissipates vibration energy, achieving highly effective vibration isolation^[7].
- To address noise and micro vibrations induced by working fluid flow within the collector tubes, plate-shaped stabilizing devices can be installed at the condensing end with progressively increasing spacing to optimize the flow field and suppress vortex formation^[8].

4.1.2 Installation Solutions for Component and Safety Devices

In engineering practice, the proper installation of various components and safety devices in siphon-type solar water heating systems is essential for ensuring the system operates normally, safely, and efficiently. Below are some recommendations drawn from practical engineering experience.

- To address stresses caused by thermal expansion and contraction, compensation measures must be systematically integrated into the piping system, with the compensation capacity calculated based on the thermal expansion coefficient of the pipe material and the maximum temperature differential. At equipment interfaces, metal braided hoses should be used for transitions, with lengths no less than three times the pipe diameter and installed in a natural state without stretching or compression.
- The support system should combine sliding supports and guide supports, with polytetrafluoroethylene (PTFE) pads on sliding supports having a friction coefficient below 0.1 to ensure free pipe movement. During system commissioning, a thermal alignment check must be performed by heating the system to operating temperature and re-inspecting all supports to verify proper compensator function.
- If the installation area experiences frequent lightning strikes, lightning protection devices should be installed for the collector and water tank. These devices should be connected via insulated components to safely ground the lightning current.
- Pressure relief valves must be installed at the pressurized thermal storage unit to promptly release pressure during abnormal pressure surges, ensuring container safety. To counter severe weather such as hail, motor-driven retractable protective panels can be installed above the collector array. These panels deploy rapidly during hail events to shield vacuum collector tubes^[9]. Alternatively, physical isolation can be achieved through metal hail protection netting (note this approach incurs loss in solar radiation energy).
- All exhaust or overflow ports must always remain unobstructed. Blockage is strictly prohibited to prevent damage to the water tank caused by abnormal pressure.

4.2 Multi-layered Protection System

An effective multi-layered safety protection system should cover critical stages from heat collection and storage to piping. Through the coordinated use of structural design, intelligent control, and mechanical safety devices, it must address multiple risks including overheating, freeze damage, heat loss, and corrosion.

4.2.1 Overheating Protection

Currently, the overheating issue in siphon-type solar water heaters is primarily addressed through strategies such as improving system structural design, integrating overheating protection devices, and utilizing phase change thermal storage materials. The following are some specific solutions:

To prevent overheating from summer sun exposure, heat-collecting tubes with built-in phase change materials (PCM) can be employed. For instance, a solid-liquid phase change material with a transition temperature of 40-60°C can be placed between the inner sleeve and the evaporation end of the heat pipe. By absorbing heat through melting, it smooths out temperature peaks, protects the heat-absorbing coating, and slows the rise in system pressure^[10].

By minimizing fluid filling and intentionally operating near the 'dry limit', the system maintains traditional efficiency levels at operating temperatures up to 80 °C and limits stagnation temperature to 95 °C under high irradiance summer conditions^[1].

4.2.2 Frost Protection

Research on freeze protection for siphon-type solar water heaters has developed multiple technical approaches. The core concept involves addressing low-temperature risks through passive design or material applications, aiming to achieve maintenance-free, efficient, and reliable system operation.

Connect the solar water heater tank, L-shaped pipe, inlet/outlet pipes, auxiliary pipes, auxiliary sealing box, check valve, and multiple valves in a specific sequence. Maintain a constant volume of water within the auxiliary sealing box. Utilize the siphon principle to access hot water from the solar water heater tank and drain water from the pipes. By solely improving the physical structure without consuming electricity, this system ensures the solar water heater functions normally during freezing seasons. Additionally, the system remains unaffected by pipe scaling issues^[11].

By adding an additional circulation loop connected to the heat source below the collector, it utilizes density changes caused by water temperature differences to achieve natural circulation, thereby preventing freezing^[4].

By integrating supercritical CO₂ with thermosiphon vacuum tube collectors, the system operates normally without freezing at low temperatures, overcoming the technical bottleneck of solar water heating systems in severely cold regions^[3].

4.2.3 Comprehensive Corrosion Protection Solutions

Corrosion prevention solutions for thermosiphon solar water heaters primarily focus on material innovation, structural design optimization, and electrochemical protection, aiming to enhance system durability in complex water quality environments.

- At the water treatment stage, online water quality monitors should track chloride ion concentration, activating softening processes when Cl⁻ levels exceed 100 mg/L. In high-risk areas, materials like duplex stainless steel 2205 or titanium are advised for inner tanks.
- Cathodic protection should combine traditional magnesium sacrificial anodes with an Impressed Current Cathodic Protection (ICCP) system.
- Regular maintenance must include endoscopic inspections of tank interiors, focusing on weld-affected zones and deformed areas to detect micro-cracks early.
- A corrosion database logging inspection results enable big-data analysis for predicting equipment remaining life.

4.2.4 Intelligent Insulation System Design

The performance of the insulation system directly impacts thermal efficiency.

Prefabricated polyurethane insulation shells should be used for collector pipes, with thicknesses (typically ≥ 50 mm) determined via heat loss calculations. The insulation exterior must be covered with 0.5 mm aluminum sheeting, all seams joined by crimping and sealed with silicone. Storage tanks require monolithic foam insulation, with foam density reaching 40 kg/m³ and a closed-cell rate exceeding 90%. Notably, all valves, flanges, and accessories should feature removable insulation structures for easy maintenance. To monitor insulation effectiveness in real time, temperature sensors embedded within the insulation can trigger alerts if surface-to-ambient temperature differentials exceed limits. Quarterly infrared thermographic scans of the entire system are recommended to detect and address insulation defects promptly.



4.3 Intelligent Monitoring and Predictive Maintenance Systems

4.3.1 Monitoring Platform Development

A smart monitoring system forms the foundation for predictive maintenance. A multi-sensor network—including PT100 temperature sensors ($\pm 0.1^\circ\text{C}$ accuracy), pressure transmitters (0.5% accuracy), and electromagnetic flow meters (0.2% accuracy) should collect data every 5 minutes, with critical parameters like collector outlet temperature uploaded in real time to a cloud platform. The platform software must incorporate machine learning to establish normal operating models based on historical temperature-pressure-flow correlations, triggering alerts when real-time data deviates by more than 3σ . Integration of weather forecast data allows 24-hour prediction of solar energy gain, optimizing auxiliary heating operation strategies.

4.3.2 Implementation of Predictive Maintenance Strategies

Predictive maintenance leverages monitoring data for precision interventions. An Equipment Health Index (EHI) system should encompass efficiency metrics (e.g., collector efficiency decay rate), reliability indicators (e.g., mean time between failures), and economic factors (e.g., maintenance cost rate). Time-series analysis algorithms can forecast performance degradation, such as predicting pump bearing remaining life via vibration frequency changes. Maintenance schedules should evolve from fixed intervals to condition-based actions. A mobile app enables field technicians to access historical data, maintenance records, and repair guides in real time, boosting efficiency. A knowledge base system accumulating maintenance experiences, supported by case-based reasoning, provides solutions for novel faults.

Through systematic implementation of these technical solutions, the reliability and service life of thermosiphon solar water heating systems can be significantly enhanced. All measures must be grounded in detailed engineering calculations and on-site testing, tailored to specific project conditions. A robust technical documentation management system is recommended to support full lifecycle data management.

5 Conclusion

Currently, thermal siphon solar collectors face severe challenges in durability and reliability during long-term operation, with core issues centered on material aging, environmental corrosion, system overheating, nighttime heat loss, and freezing in severe cold. Research indicates that deterioration of sealant performance and insulation failure are the primary causes of significant decline in system thermal performance, while overheating and freezing directly threaten system safety and lifespan.

To address these challenges, technological development is shifting from traditional passive protection toward a new paradigm of intelligent prediction and active regulation. This shift has spawned multiple innovative solutions, such as achieving self-limiting overheating protection through precise management of working fluids, utilizing phase change materials to suppress heat loss, and employing novel working fluids combined with passive anti-freeze designs to overcome application bottlenecks in frigid regions. Simultaneously, system reliability increasingly relies on comprehensive technical measures including vibration-resistant design, multi-tiered corrosion prevention systems, and data-driven predictive maintenance. This shift signifies a strategic transition in the field—moving beyond the singular pursuit of initial efficiency toward a holistic enhancement of full-lifecycle performance and reliability.

Looking ahead, the development of thermosiphon solar technology will increasingly focus on optimizing performance throughout its entire lifecycle, enhancing reliability, and achieving harmonious coexistence with the environment. Its evolution will follow three major trends: First, deep intelligence, where artificial intelligence and Internet of Things technologies will be deeply integrated, enabling systems to make adaptive decisions and perform proactive operations and maintenance based on multi-source information (such as weather forecasts and user habits), becoming true “smart energy units.” Second, continuous innovation in materials and structures. The application of next-generation advanced functional materials—such as phase-change materials, nano-insulation materials, and self-healing coatings—will fundamentally enhance the system's thermal management capabilities, durability, and environmental adaptability. Third, system integration and multifunctionality. Solar water heating systems will no longer operate as standalone devices but become integral components of building energy systems.

They will deeply integrate with photovoltaic-thermal hybrid systems, space heating, and other technologies to achieve cascaded energy utilization and maximize efficiency.

Through the comprehensive application of the technologies, future thermosiphon solar systems will achieve “maintenance-free” or “minimal-maintenance” reliable operation across a broader range of climatic zones, from the equator to the polar regions. Ultimately, the development of this technology will transcend the singular pursuit of initial efficiency, instead striving to become a robust, reliable, and intelligent cornerstone in building the sustainable energy systems of the future.



6 Appendix

6.1 Abbreviations

SHW	Solar Hot Water
GHG	Greenhouse Gas
GN-SEC	Global Network of Regional Sustainable Energy Centres
R&D	Research and Development
T&P Valves	Temperature and Pressure Relief Valves
LSTM	Long Short-Term Memory
AI	Artificial Intelligence
PCMs	Phase Change Materials
GA	Genetic Algorithms
ANN	Artificial Neural Networks
COP	Coefficient Of Performance
FPC	Flat-Plate Collector
GSETC	Glass-metal Sealed Evacuated Tube Collector
HPETC	Heat Pipe Evacuated Tube Collector
UETC	U-type Evacuated Tube Collector
ETC	Evacuated Tube Collector
AGETs	All-Glass Evacuated Tubes
LT	Loop Thermosyphon
SWH	Solar Water Heating
LT-SWH	Loop Thermosyphon Solar Water Heating
EGT	Evacuated Glass Tube
NRV	Non-Return Valve
PCM	Phase Change Material
DIY	Do It Yourself
PTFE	Polytetrafluoroethylene
CFD	Computational Fluid Dynamics
ICCP	Impressed Current Cathodic Protection
EHI	Equipment Health Index

6.2 List of Figures

Figure 1: Typical product failure rate curve.

Figure 2: Market Share of ETC and FPC in China.

Figure 3: Images of Some ETCs after Exposure.

Figure 4: Thermal Performance Change of FPC.

Figure 5: Thermal Performance Change of GSETC.

Figure 6: Thermal Performance Change of HPETC.

Figure 7: Thermal Performance Change of UETC.

Figure 8: Ephesus Thermosiphon Solar Water Heater with 24 AGETs and Schematic Diagram of The Solar Simulator Set up for The Conditioned Medium Used in The Field Experiments.

Figure 9: Solar Simulator Test Results.

Figure 10: Solar Heating Efficiencies.

Figure 11: Longitudinal Division of New Storage Tank.

Figure 12: Total Solar Irradiance on The Surface of Thermosyphon and Ambient Temperature for A Particular Day 1st of January, March, and July.

Figure 13: Temperature Variation of The Water Flowing into The Storage Tank from The Collector for A Particular Day (1st of January, March, and July).

Figure 14: Variation of Water Temperature inside The Classic Tank.

Figure 15: Experimental Temperature Variation of The Phase Change Material in The Charging Phase.

Figure 16: Experimental Temperature Variation of the Phase Change Material in The Discharging Phase.

Figure 17: Temperature Variation of Water inside The New and Classic Thermosyphon Tanks on A (a) Summer Day (b) Winter Day.

Figure 18: The Comparison of The Current Results with Experimental and Published Data on A (a) Summer Day and (b) Winter Day.

Figure 19: Thermal Fields in The Charging Phase.

Figure 20: Thermal Fields in Discharging Phase.

Figure 21: Front and Rear View of Solar Water Heating System with CO₂ Filling Circuit.

Figure 22: Climate of Gilgit-Baltistan (Pakistan).

Figure 23: The Result of Serpentine and Parallel U Tube Arrangements in Solar Water Heater.

Figure 24: Blockage of NRV Due to Dry Ice CO₂.

Figure 25: Innovative Design of Manifold with U Shaped Copper Tubes.

Figure 26: Variation of Collector Output Temperature and Pressure from 7 AM to 16 PM.

Figure 27: Useful Heat Gain and Efficiency of System.

Figure 28: Performance of Solar Water Heating System During a Mild Sunny Day.

Figure 29: Dual Loop Thermosyphon.

Figure 30: Classic Thermosyphon.

Figure 31: Daytime Operation.

Figure 32: Nighttime Operation.

Figure 33: Solar Collectors.

Figure 34: Classic Thermosyphon Pipes above The Collectors.

Figure 35: Lower Loop Connects to Buried Coil.

Figure 36: Schematic Diagrams of LT-SWH System and Conventional SWH System.

Figure 37: Variations in Monthly Average Ambient Temperature, R_b , Monthly Cumulative Solar Radiation.

Figure 38: Comparison of The Monthly Effective Numbers under Different Heating Modes.

Figure 39: Comparison of The Monthly Effective Heat Gains of Supplying Days under Different Heating Modes.

Figure 40: Comparison of Monthly Cumulative Heat Loss and Monthly Average Temperature Drops.

Figure 41: Comparison of Heat Loss Ratios under Different Heating Modes.

Figure 42: Comparison of Monthly Average Thermal Efficiencies under Different Heating Modes.

Figure 43: Variation of The Effective Number of Supplying Heat Gain Days with Final Water Temperature.



Figure 44: Variation of The Annual Cumulative and Temperature Drop with The Increasing Set.

Figure 45: Variations of The Average Annual Temperature Water Rise, and Temperature Drop with The Increasing Set Temperature.

Figure 46: Variations of The Average Annual Initial Temperature and Final Water Temperature with Increasing Set Temperature.

6.3 List of Tables

Table 1: Specification of Tested Flat Plate Solar Collector.

Table 2: Specifications of The Tested Evacuated Tube Collectors.

Table 3: Test Conditions.

Table 4: Thermal Performance Before and After Test (Based on Inlet Temperature, Aperture Area).

Table 5: Specifications of Thermal Storage Tank.

6.4 References

- [1] Mert Çimen, Mehmet Colakoglu, Ali Güngör, Overheating limitation of thermosyphon solar collectors by controlling heat pipe fluid in all glass evacuated tubes, *Solar Energy*, 2021(230):515-527.
- [2] Sami Awani, Ridha Chargui, Bourhan Tashtoush, Experimental and numerical evaluation of a new design of a solar thermosyphon water heating system with phase change material, *Journal of Energy Storage*, 2021(41):102948.
- [3] N. Abas, N. Khan, A. Haider, M.S. Saleem, A thermosyphon solar water heating system for sub zero temperature areas, *Cold Regions Science and Technology*, 2017(143):81-92.
- [4] Stayton, R. (2023). Passive Freeze Protection for Thermosyphon Water Heating. In: Renné, D., Rixham, C., Reddington, L. (eds) *Proceedings of the 52nd American Solar Energy Society National Solar Conference 2023. ASES SOLAR 2023*. Springer Proceedings in Energy. Springer, Cham. https://doi.org/10.1007/978-3-031-39147-7_12
- [5] T. Zhang, Z.W. Yan, L.Y. Wang, et al. Comparative study on the annual performance between loop thermosyphon solar water heating system and conventional solar water heating system, *Solar Energy*, 2020(197):433-442.
- [6] Zhang Hailing. Sliding-Type Solar Thermal Collector with Anti-Vibration Structure[P]. China: CN114234457B, 2022.
- [7] Zhejiang Provincial Architectural Design and Research Institute. Seismically Isolated Hybrid Energy Water Heater[P]. China: 201410392640, 2014.
- [8] Weihai Wenhai Energy-Saving Technology Co, Ltd. A Solar Water Heater with Variable Spacing of Condenser-End Stabilizing Devices[P]. China: CN110631266B, 2020.
- [9] Bao Hongxi. A Patent for a Solar Water Heater with Adjustment Functionality and High Safety and Reliability[P]. China: CN110887254A, 2020.
- [10] Beijing Tongchuang Luyuan Energy Technology Co., Ltd. A Patent for a High-Safety Heat-Absorbing Method for Collector Tubes[P]. China: CN113669921B, 2024.
- [11] Li Xiaomeng. Solar Water Heater Anti-Freeze System[P]. China: 201320761457.5, 2013.